archives
of thermodynamics
Vol. **40**(2019), No. 3, 123–136
DOI: DOI: 10.24425/ather.2019.129997

Hydraulic resistance analyses of selected elements of the prototype Stirling engine

MARIUSZ FURMANEK
JACEK KROPIWNICKI*

Gdańsk University of Technology, Faculty of Mechanical Engineering,
Narutowicza 11/12, 80-233 Gdańsk, Poland

Abstract The paper presents the results of simulation tests of hydraulic resistance and temperature distribution of the prototype Stirling alpha engine supplied with waste heat. The following elements were analyzed: heater, regenerator and cooler. The engine uses compressed air as a working gas. Analyses were carried out for three working pressure values and different engine speeds. The work was carried out in order to optimize the configuration of the engine due to the minimization of hydraulic resistance, while maintaining the required thermal capacity of the device. Preliminary tests carried out on the real object allowed to determine boundary and initial conditions for simulation purposes. The simulation assumes that there is no heat exchange between the regenerator and the environment. The solid model used in simulation tests includes the following elements: supply channel, heater, regenerator, cooler, discharge channel. Due to the symmetrical structure of the analyzed elements, simulation tests were carried out using 1/6 of the volume of the system.

Keywords: Stirling engines; Temperature distribution; Hydraulic resistance

1 Introduction

The development of technology poses new challenges for the power industry by forcing the improvement of existing solutions, the recovery of energy from undeveloped carriers and the search for alternative energy sources.

*Corresponding Author. Email: jkropiwn@pg.gda.pl

One of such renovated technology is the Stirling engine [1–3], namely the external combustion engine. Nowadays Stirling engines are mostly used in electric power production systems for households [4–8]. As a heat source the waste heat from technological processes can be used or the heat generated during combustion of low caloric fuel [9,10]. Unconventional energy sources can be the energy carrier for the Stirling engine, e.g., biomass, geothermal and solar energy [11]. This solution enables operation with low-temperature medium (120–150 °C) and high-temperature medium (above 700 °C) [12–15]. The variety of energy sources makes it an alternative to conventional power systems [16–19]. The Stirling engine is characterized by high efficiency (similarity to the Carnot cycle) and simple construction (no valve-train) [20–22]. The uncomplicated design increases reliability and simplifies maintenance. The biggest disadvantage of the engine is the high price for small scale industrial applications. The most expensive elements in the systems are heat exchangers. Gases used as a working fluid have a lower heat transfer properties in comparison to liquids. To maintain the same amount of heat supplied to the system some modifications are expected, e.g., increasing the heat exchange surface or intensify the heat exchange process itself [17,23].

A prototype of the Stirling alpha engine (diameter/stroke: 0.13/0.055 m) was developed in the laboratory of Gdańsk University of Technology (Fig. 1). The engine can be driven by mid-high temperature waste gases coming from internal combustion engine. The engine performance was tested with air as the working gas at charged pressure 200–500 kPa and heating temperature of 200–400 °C.

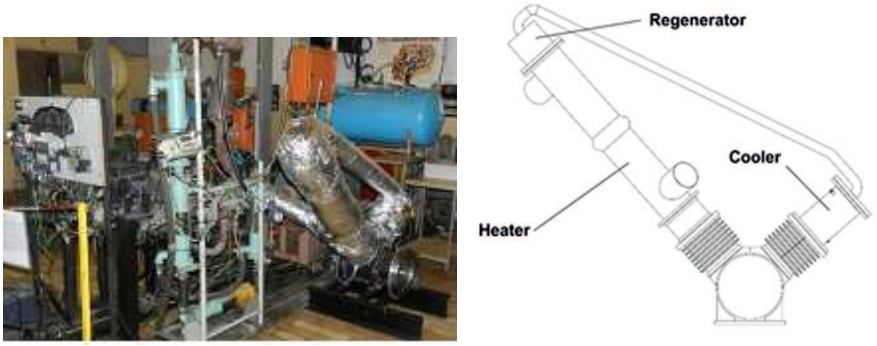

Figure 1: Prototype Stirling alpha engine powered by exhaust gasses from internal combustion engine.

Obtained results were not satisfactory, indicated work for the supply temperature 210 °C and the average pressure of 230 kPa was 2.3 J and successively increased with the temperature and charging pressure up to 13 J. Pressure loss in the selected elements of the Stirling engine was tested out in the laboratory of the Faculty of Mechanical Engineering of the Gdańsk University of Technology on a separate test bench [24]. Tests were performed for the one way fixed flow using the air compressor as a source of flow (Fig. 2). The apparatus measurement uncertainty used in the tests has been presented in Tab. 1.

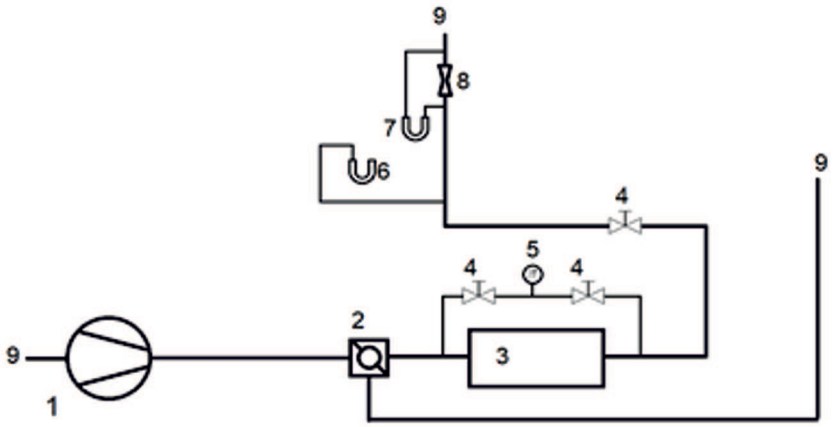

Figure 2: Diagram of the pressure loss measurement system: 1 – air compressor, 2 – three-way valve, 3 – tested elements, 4 – shut-off valve, 5, 6, 7 – manometer, 8 – measuring orifice, 9 – atmosphere [24].

Table 1: Apparatus measurement uncertainty.

Parameter	Measurement uncertainty
Pressure	72 Pa
Temperature	1.5 °C
Mass flow rate	1.8×10^{-4} kg/s (2%)

Measured at the test bench pressure loss for the 3 main components: heater, regenerator, cooler, achieved 1.56 kPa for the mass flow rate corresponding to the 250 rpm. The registered value was unsatisfactory, in particular, with

the increase of the charging pressure and the engine speed, a rapid increase in hydraulic resistance was recorded.

It was estimated that for a pressure of 460 kPa the sum of hydraulic and mechanical resistance is 17 J. Unfortunately the indicated power did not exceed the total resistance in any tested point of operation. To start the engine, it is necessary to increase the indicated work or significantly reduce resistance. The assumed target engine operating parameters (1000 kPa charging pressure, 750 rpm) would therefore cause too large hydraulic resistance in the system. As a result, designed prototype was modified due to reduction of hydraulic resistance. Figure 3 presents a Stirling engine design with a more compact construction with a limited number of regenerator fillings made of metal mesh and a reduced length of pipelines connecting individual engine components.

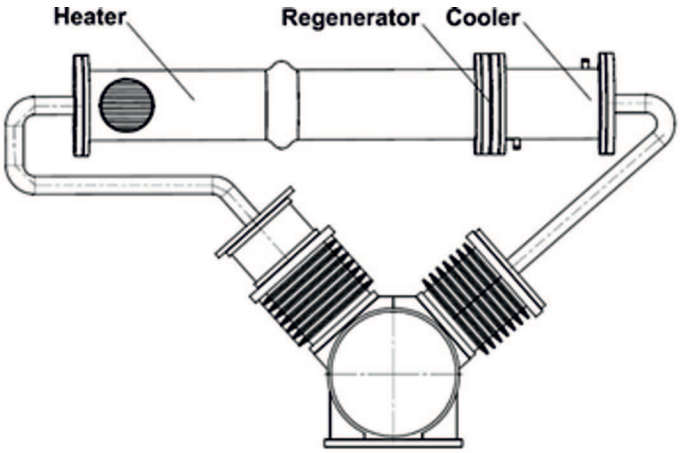

Figure 3: Design of Stirling engine alpha type after modifications.

Presented work describes undertaken effort to reduce hydraulic resistance of the analyzed Stirling engine elements. The following sections present the results of simulation tests of pressure and temperature distribution of the prototype Stirling engine alpha type supplied with waste heat. The following elements were analyzed: heater, regenerator and cooler. The engine uses compressed air as a working gas. Analyses were carried out for three working pressure values and four engine speeds. The engine rotational speed is directly related to the mass flow rate via piston speed. Assumed in calculations mass flow rates of the working fluid are corresponding to

the piston mean speed for the selected engine rotational speed. The work was carried out assuming that the required thermal capacity of the device is maintained.

2 Hydraulic resistance analysis of selected elements

Preliminary tests carried out on the real object allowed to determine boundary and initial conditions for simulation purposes, i.e.: average mass flow rate, temperature and air pressure at the inlet to the heater. The simulation assumes that there is no heat exchange between the regenerator and the environment. As a part of the identification of the operating conditions of the Stirling engine, the temperature of the flue gas flowing through the heater as well as the temperature of the water receiving the heat from the cooler were also measured on the test bench. Table 2 contains initial conditions, whereas boundary conditions are included in Tab. 3.

Table 2: Initial conditions of the simulation.

Location	Parameter	Value
Inlet	Temperature	170 °C
	Pressure	200 kPa, 300 kPa, 400 kPa
Outlet	Mass flow rate	Resulting from the mean piston speed and the pressure

It should be emphasized that the performed simulation relates to one-way fixed flow. That is significant simplification of the process occurring in the real Stirling engine, which is characterized by the periodic nature of work [25–29]. It can be expected that for dynamic process, such as pressure change in engine components, such simplification does not bring significant errors, while the simulation of the temperature change in the working medium can only bring the information of a qualitative not quantitative nature. It was decided to carry out a simulation for the steady state due to the possibility of assessing the impact of the new design solutions on hydraulic resistance, the measure of which is the pressure loss during the flow of the working gas through the heater, regenerator and the cooler. The

Table 3: Boundary conditions of the simulation.

Location	Condition
Cooler	Boundary condition of a third kind, heat transfer coefficient of radiator – $u_r = 71.27\ \frac{W}{m^2K}$ Temperature of cooling water – $t_w = 55\,^\circ C$
Heater	Boundary condition of a third kind, heat transfer coefficient of heater – $u_h = 13.82\ \frac{W}{m^2K}$ Temperature of exhaust gases – $t_{ex} = 320\,^\circ C$
Regenerator and other surfaces	Boundary condition of third kind – adiabatic process

first variant of the engine was tested due to the hydraulic resistance on the test bench (Fig. 2) with a steady flow and the results of these tests could be used as a reference level.

Figure 4 shows the solid model used in simulation tests. It was developede using the commercial Autodesk Inventor CAD software [30]. Heat exchangers (cooler and heater) consist of 121 tubes with outside diameter of 0.4 m. The linear dimension of the cooler is 0.21 m, the length of the heater is 0.75 m.

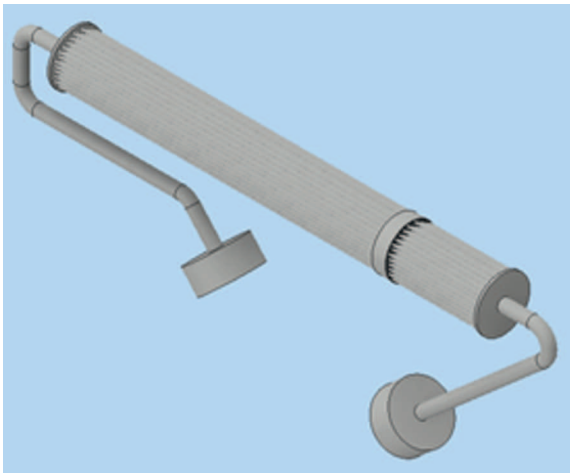

Figure 4: 3D geometry of the Stirling engine type alpha.

The solid model used in simulation tests includes the following elements:

supply channel, heater, regenerator, cooler and discharge channel. Due to the symmetrical structure of the analyzed elements, simulation tests were carried out using 1/6 of the system's volume. Figure 5 shows 1/6 of the exchanger system. Due to symmetrical shape of the designed elements it is possible to use a grid with fewer elements.

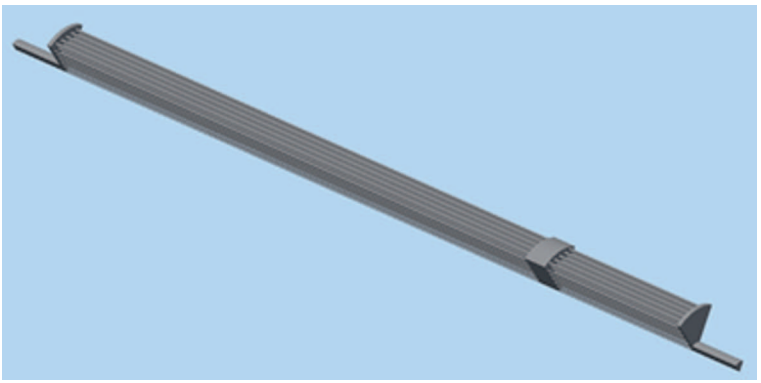

Figure 5: The analyzed elements: heater, regenerator and cooler – 1/6 of the total volume.

Numerical calculations have been carried out in commercial engineering simulation software package Ansys [31] for the heater, regenerator and radiator system in various speed configurations. Variable quantities are pressure and mass flow resulting from the rotational speed. Having the appropriate number of simulations, it is possible to determine the impact of selected parameters on the amount of pressure losses. Knowledge about the influence of any parameters on hydraulic resistance is crucial when designing elements such as cooler and heater. Figures 6, 7, and 8 show the pressure and temperature distribution in the analyzed elements for pressures of 200, 300, and 400 kPa, respectively. In Tabs. 4, 5, and 6 results of simulation have been presented, respectively for air inlet pressure 200, 300, and 400 kPa.

In Fig. 9 pressure loss *vs.* mass flow rate for air inlet pressure 200, 300, 400 kPa has been presented. The correctness of the numerical model has been verified for the specified operating point (400 kPa, 250 rpm) using analytical calculation, basing on coefficients taken from literature. In the case under consideration, the pressure loss obtained from simulations and from analytical calculations read respectively 0.98 kPa and 1.03 kPa. The resulting difference is very small and amounts to only 5%, which indicates

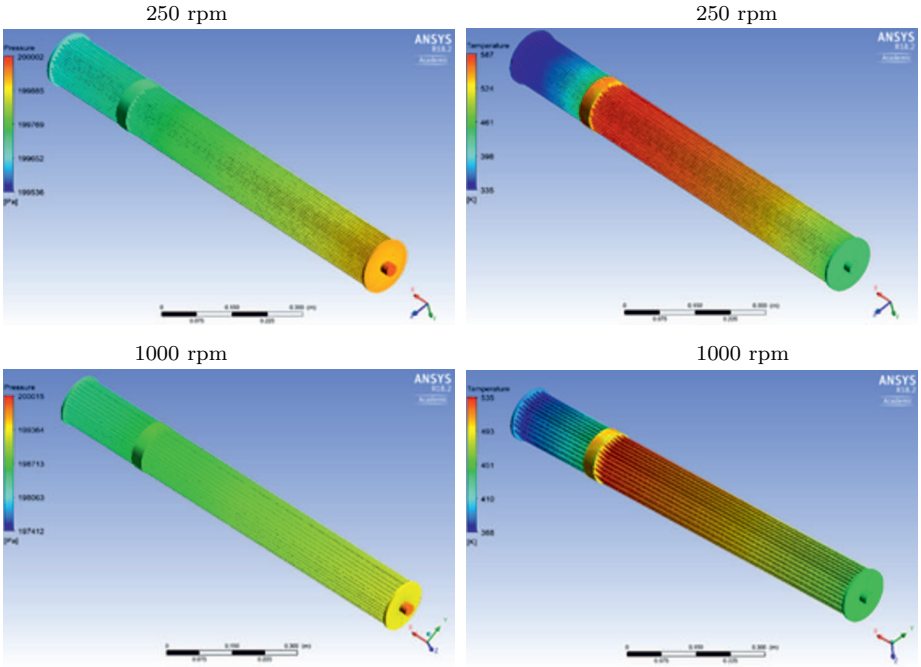

Figure 6: Pressure (left) and temperature (right) distribution for the pressure inlet 200 kPa.

Table 4: Pressure loss for charging pressure 200 kPa.

Engine speed	Mass flow rate	Inlet pressure	Outlet pressure	Pressure loss
rpm	kg/s	kPa	kPa	kPa
250	0.0046	199.97	199.59	0.38
500	0.0092	199.91	198.93	0.98
750	0.0138	199.78	197.84	1.94
1000	0.0184	199.60	196.40	3.20

the correctness of the numerical model used.

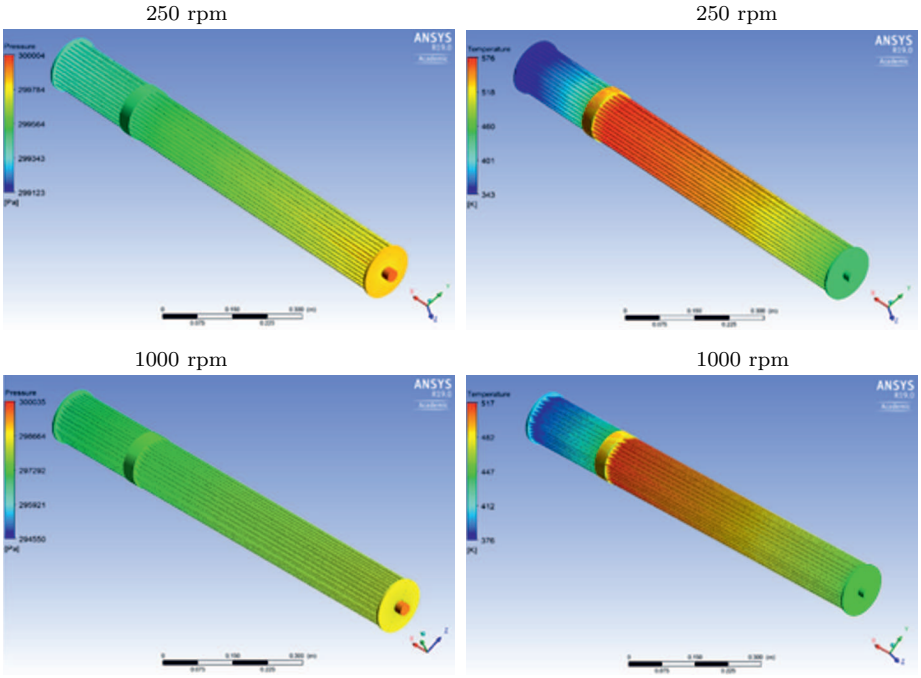

Figure 7: Pressure (left) and temperature (right) distribution for the pressure inlet 300 kPa.

Table 5: Pressure loss for charging pressure 300 kPa.

Engine speed	Mass flow rate	Inlet pressure	Outlet pressure	Pressure loss
rpm	kg/s	kPa	kPa	kPa
250	0.0069	299.94	299.24	0.70
500	0.0138	299.78	297.84	1.94
750	0.0207	299.50	295.54	3.96
1000	0.0276	299.14	292.70	6.44

3 Results

In the analyzed cases (Figs. 6–8), as a result of increasing the charging pressure at 250 rpm, the maximum temperature in the heater decreased from 587 °C to 567 °C. Similarly, at 1000 rpm the maximum temperature in the heater decreased from 535 °C to 505 °C. By increasing the charging

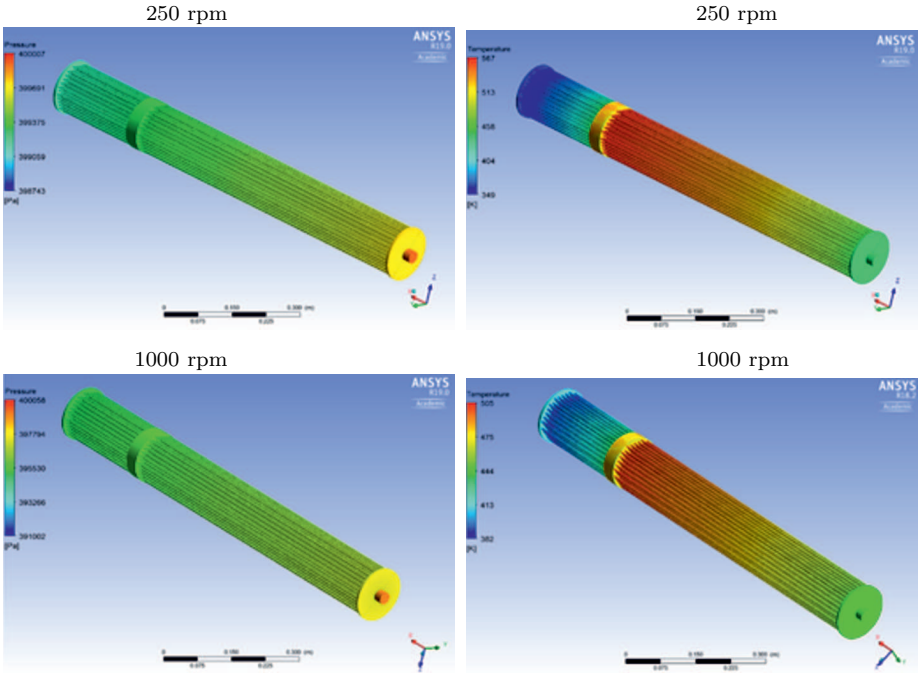

Figure 8: Pressure (left) and temperature (right) distribution for the pressure inlet 400 kPa.

Table 6: Pressure loss for charging pressure 400 kPa.

Engine speed]	Mass flow rate	Inlet pressure	Outlet pressure	Pressure loss
rpm	kg/s	kPa	kPa	kPa
250	0.0092	399.91	398.93	0.98
500	0.0184	399.61	396.39	3.22
750	0.0276	399.14	392.70	6.44
1000	0.0368	398.48	387.70	10.79

pressure, the mass flow rate is increased, thereby the working gas heat capacity is raised up, which causes lowering the air temperature at the end of the heating process and increasing the air temperature in the cooler. The increase of the rotational speed contributes to the increase of the linear speed of the medium, the effect is a shorter contact time of the working medium with the walls, causing the same consequences as it happens after

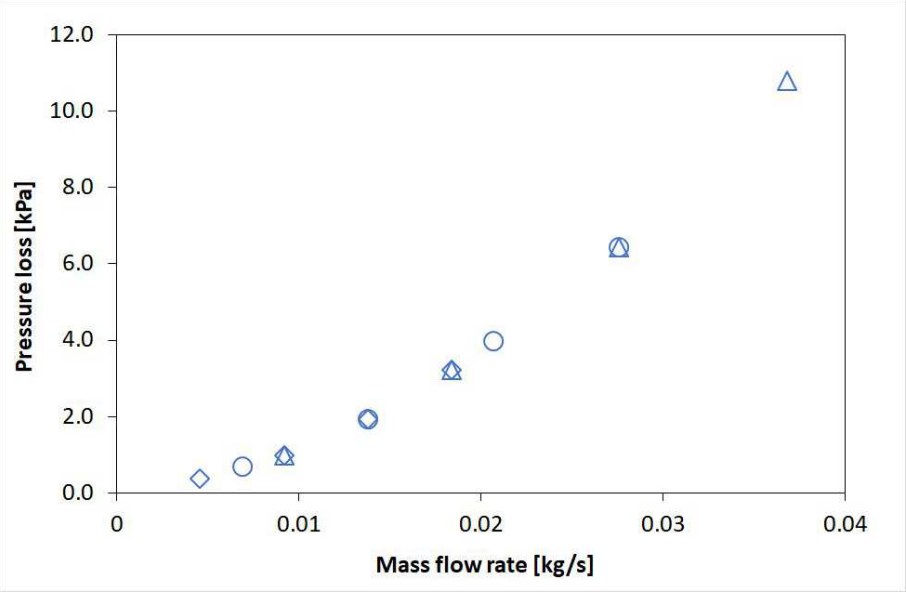

Figure 9: Pressure loss *vs.* mass flow rate for air inlet pressure: ◇ – 200 kPa, ○ – 300 kPa, △ – 400 kPa.

the increase in pressure. The increase of pressure and rotational speed is associated with the potential increase of indicated power in the Stirling engine, but it contributes also to the reduction of the temperature difference of the working medium in the processes of expansion and compression, has a later potential effect on reducing the thermal efficiency of the device.

Presented characteristics (Fig. 9) cover the target speed range of the prototype device. In the analyzed cases, as a result of increasing the engine speed and consequently increasing mass flow rate of the working fluid, the pressure loss is rising from 0.38 to 3.20 kPa for 200 kPa charging pressure, and up to 10.79 kPa for 400 kPa charging pressure.

4 Conclusions

The paper presents the results of simulation tests of pressure and temperature distribution in the prototype Stirling engine alpha type supplied with the waste heat. The following elements were analyzed: heater, regenerator and cooler. The work was carried out in order to minimize the hydraulic resistance of the device, while maintaining the required heat delivery. The

performed simulation relates to the one-way fixed flow. That is significant simplification of the process occurring in the real Stirling engine, which is characterized by the periodic nature of work. It can be expected that for dynamic process, such as pressure change in engine components, such simplification does not bring significant errors, while the simulation of the temperature change in the working medium can only bring the information of a qualitative not a quantitative nature.

For the Stirling engine operating conditions registered during the prototype tests, the pressure loss in the engine after modification is 0.98 kPa. As a result of modification, there was a reduction in the pressure loss compared to the previous version of the engine by 37%. It can be therefore concluded that the structural changes, made in the prototype, have significantly reduced the hydraulic resistance in the main engine's components. In the last analyzed case, corresponding to the highest power produced by the engine, the calculated hydraulic resistance is 98 W, which is still significant share of the total resistance (hydraulic and mechanical) of 304 W (the same point of operation).

Received 23 November 2018

References

[1] Walker G.: *Stirling Engines*. Oxford University Press, 1980.

[2] Żmudzki S.: *Stirling Engines*. WNT, Warszawa 1993 (in Polish).

[3] Finkelstein Th., Organ A.J.: *Air Engines*. ASME, New York 2001.

[4] Buoro D., et al.: *Optimal synthesis and operation of advanced energy supply systems for standard and domotic home*. Energ. Convers. Manage. **60**(2012), 96–105.

[5] Bernd Th.: *Benchmark testing of Micro-CHP units*. Appl. Therm. Eng. **28**(2008), 2049–2054.

[6] Gianluca V., et al.: *Experimental and numerical study of a micro-cogeneration Stirling engine for residential applications*. Energy Procedia **45**(2014), 1235–1244.

[7] Li T., et al.: *Development and test of a Stirling engine driven by waste gases for the micro-CHP system*. Appl. Therm. Eng. **33-34**(2012), 119–123.

[8] Remiorz L, et al.: *Comparative assessment of the effectiveness of a free-piston Stirling engine-based micro-cogeneration unit and a heat pump*. Energy **148**(2018), 134–147.

[9] Marion M., Hasna L., Gualous H.: *Performances of a CHP Stirling system fuelled with glycerol*. Renew. Energ. **86**(2016), 182–191.

[10] Meybodi M., Behnia M.: *Australian coal mine methane emissions mitigation potential using a Stirling engine-based CHP system*. Energy Policy **62**(2013), 10–18.

[11] Lane N.W., Beale W.T.: *A Biomass-fired 1 kWe Stirling engine generator and its applications in South Africa*. In: Proc. 9th Int. Stirling Engine Conf., South Africa, June 2–4, 1999.

[12] Cheng C.H., et al.: *Theoretical and experimental study of a 300-W beta-type Stirling engine*. Energy **59**(2013), 590–599.

[13] Karabulut H., et al.: *An experimental study on the development of a b-type Stirling engine for low and moderate temperature heat sources*. Appl. Energ. **86**(2009), 68–73.

[14] Kongtragool B., Wongwises S.: *Performance of low-temperature differential Stirling engines*. Renew. Energ. **32**(2007), 547–566.

[15] Sripakagorn A., Srikam C.: *Design and performance of a moderate temperature difference Stirling engine*. Renew. Energ. **36**(2011), 1728–1733.

[16] Kropiwnicki J.: *Design and applications of modern Stirling engines*. Combust. Engines **3**(2013), 243–249.

[17] Maier Ch., et al.: *Stirling Engine*. University of Gävle, Gävle 2007.

[18] Cieśliński J., Kropiwnicki J., Kneba Z.: *Application of Stirling engines in micro-co-generation*. In: District Heating, Heating, Renewable Energy Ssources (W. Zima, D. Taler), Wydaw. Politechniki Krakowskiej, Kraków 2013, 47–60 (in Polish).

[19] Cieśliński J., Kropiwnicki J., Kneba Z., Woronkin S., Witanowski Ł., Zalewski K.: *Investigation of a Stirling engine as a micro-CHP system*. In: Proc. 3rd Int. Conf. Low Temperature and Waste Heat Use in Energy Supply Systems Theory and Practice, Bremen 2012, 33–38.

[20] Gheith R., Aloui F., Ben Nasrallah S.: *Experimental investigation of a Gamma Stirling engine*. Int. J. Energy Res. **37**(2013), 1519–1528.

[21] Tavakolpour-Saleh A.R., et al.: *A novel active free piston Stirling engine: Modeling, development, and experiment*. Appl. Energ. **19**(2017), 9, 400–415.

[22] Kwankaomeng S., et al.: *Investigation on stability and performance of a free-piston Stirling engine*. Energy Procedia **52**(2014), 598–609.

[23] Kropiwnicki J., Furmanek M.: *The use of Stirling engine for energy recovery from flue gas*. Autobusy, Technika, Eksploatacja, Systemy Transportowe **9**(2018), 89—92 (in Polish).

[24] Kropiwnicki J.: *Stirling engines powered by renewable energy sources*. In: Proc. 22nd Int. Symp. Research-Education-Technology, Bremen 2015, 231–237.

[25] Pudlik W.: *Heat Transfer and Heat Exchangers*. Wydawn. Politechniki Gdańskiej, Gdańsk 2012 (in Polish).

[26] Madejski J.: *Theory of Heat Transfer*. Wydawn. Politechniki Szczecińskiej, Szczecin 1998 (in Polish).

[27] Tanaka M., Yamashita C.F.: *Flow and the heat transfer characteristics of Stirling engine in an oscillating flow*. JSME Int. J. **33**(1990), 2, 283–289.

[28] Uchman W., Remiorz L., Kotowicz J.: *Economic effectiveness evaluation of the free piston Stirling engine-based micro-combined heat and power unit in relation to classical systems*. Arch. Thermodyn. **40**(2019), 1, 71–83.

[29] Ranjan R.K., Verma S.K.: *Thermodynamic analysis and analytical simulation of the Rallis modified Stirling cycle*. Arch. Thermodyn. **40**(2019), 2, 35–67.

[30] Autodesk Inventor Tutorial, https://www.instructables.com/id/Autodesk-Inventor-Tutorial/ (accessed: June 30th 2019).

[31] Ansys Fluent Users Guide, https://www.ansys.com/products/fluids/ansys-fluent (accessed: June 30th 2019).